Jurnal Teknologi

Full Paper

SIMULATION OF ORGANIC RANKINE CYCLE THROUGH FLUEGAS TO LARGE SCALE ELECTRICITY GENERATION PURPOSE

Omid Rowshanaie[a*], Saari Mustapha[b], Kamarul Arifin Ahmad[c], Hooman Rowshanaie[d]

[a]Department of Chemical Engineering, Faculty of Engineering, Universiti Putra Malaysia, 43400 Serdang, Selangor, Malaysia
[b]Department of Chemical and Environmental Engineering, Faculty of Engineering, Universiti Putra Malaysia, 43400 Serdang, Selangor, Malaysia
[c]Department of Aerospace Engineering, Faculty of Engineering, Universiti Putra Malaysia, 43400 Serdang, Selangor, Malaysia
[d]Department of Crop Science, Faculty of Agriculture, Universiti Putra Malaysia, 43400 Serdang, Selangor, Malaysia

Article history
Received
30 July 2015
Received in revised form
30 September 2015
Accepted
31 October 2015

*Corresponding author
omid.rowshanaie@gmail.com

Graphical abstract

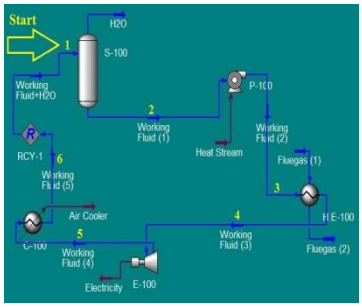

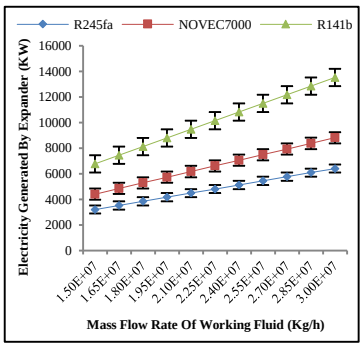

Abstract

A simulation model of Organic Rankine Cycle (ORC) was developed with HYSYS software driven by R245fa, with NOVEC7000 and R141b as working fluids and Fluegas of boilers as a heat source of shell and tube Heat Exchanger to generate large scale electricity. The initial working condition was in subcooled liquid and steady state condition. R141b was found to generate the highest electricity power increment in specific mass flow rates and inlet pressures of Expander because of approaching its critical temperature to inlet Fluegas temperature. Howeever, in terms of economic considerations and cost of shell and tube Heat Exchanger that related to total heat transfer capacity, NOVEC7000 is the optimum selection. Furthermore, R245fa has the highest total effiiciency of ORC compared with other working fluids in this study.

Keywords: Organic rankine cycle, flurgas, electricity power, working fluid.

Abstrak

Satu model simulasi bagi Kitaran Organik Rankine (ORC) telah dibangunakan dengan perisian HYSYS menerusi R245fa, dengan NOVEC7000 dan R141b sebagai cecair penggerak dan Fluegas bagi pemanas sebagai sumber haba untuk kerangka dan tiub pengubah haba bagi menjana elektrik dalam skala besar. Keadaan berkerja asal adalah dalam cecair *subcool* dan keadaan mantap. R141b dijumpai mampu menjana kuasa elektrik yang tertinggi meningkat dalam kadar aliran jisim tertentu dan tekanan inlet bagi *Expander* kerana ianya menghampiri suhu kritikal bagi suhu Fluegas inlet. Walaubagaimanapun, secara ekonominya, kerangka dan tiub pengubah haba adalah berkaitan dengan jumlah keupayaan pengalir haba, NOVEC7000 adalah pilihan yang optimum. Tambahan lagi, R245fa mengandungi jumlah kecekapan tertinggi bagi ORC berbanding cecair penggerak yang lain dalam kajian ini.

Kata kunci: Kitaran organik rankine, fluegas, kuasa elektrik, cecair penggerak

© 2015 Penerbit UTM Press. All rights reserved

1.0 INTRODUCTION

Nowadays, various governments have tried to utilize the greenhouse gases such as Fluegas produced from boilers to increase the efficiency of fuels and decrease the negative aspects of these kinds of gases such as global warming and also air pollution. As the grade of temperature of this type of gas is slightly higher, therefore it can be used in some thermodynamic effective cycles [1-3]. Toward this end, it is proposed that various thermodynamic cycles be considered. These include the Organic Rankine Cycle, Supercritical Rankine Cycle, Kalina Cycle, Goswami Cycle, Trilateral Flash Cycle, and Transcritical Rankine Cycle, which are driven by a number of refrigerant working fluids and they simulate and carry out the conversion of low-grade heat sources into electricity [4].

ORC thermodynamic cycle has a number of advantages such asL its simple structure, the availability of its components, the ease of application for local small-scale power generation systems, and driven by low-grade heat sources with temperature lower than 370^{0}C and below this temperature called low-grade temperature in industry. The structure of ORC thermodynamic cycles is similar to a typical Rankine Cycle (RC) which uses water as a working fluid, but in ORC systems the organic fluids especially refrigerant fluids are used as working fluids with high critical coordinate values, because of lower specific vaporization [5-8,2].

Pei *et al.* [9] designed and investigated an ORC thermodynamic cycle using R123 as a working fluid and turbine shaft power for generating the electricity. The electric power and cycle efficiency showed 1KW and three percent respectively. Hun investigated an ORC system by using R245fa as a working fluid and also used a radial turbine coupled with a high-speed generator designed for thermodynamic properties of working fluid used in this study. It was found that the maximum average cycle, turbine efficiencies, and electric power were 5.22%, 78.7%, and 32.7KW, respectively [10]. Baomin et al. using the Transcritical Rankine Cycle (TRC) compared a number of working fluids such as pure CO_2 and zeotropic mixtures composed of CO_2 mixed with R32, R1270, R161, R1234yf, R134a, R152a, and R1234ze according to Irreversibility and exergy of component of TRC thermodynamic cycle to produce higher electric energy [11].

This study first attempts to investigate R245fa from HFC refrigerant fluids group; secondly, it investigates NOVEC 7000 from HFE refrigerant fluids group, and thirdly, R141b is considered from HCFCs group as refrigerant working fluids, because of high heat of vaporization ($\Delta h_{vap.}$) and high density in vapor state ($\rho_{vap.}$), compared with other refrigerant fluids. An ORC thermodynamic cycle is then designed and simulated by using these refrigerant working fluids and driven by Fluegas [12]. The Fluegas, which is used in this ORC thermodynamic cycle is produced from coal, especially Bituminous coal that is used as a source of combustion fuel in boilers to produce Fluegas [13].

The majority of current researches have used the particular initial working condition such as: critical, super critical, and so on, to start the thermodynamic cycles for generating electricity at a high cost to carry out these non-simple working conditions. However, this study attempts to generate large-scale electricity that is suitable for industrial use (>3MW) by using the steady state and subcooled liquid working conditions.

This current study was carried out to evaluate the large scale electricity generated by Expander from the ORC thermodynamic cycle between R245fa, NOVEC 7000, and R141b as working fluids and driven by Fluegas and using HYSYS simulation also focused on total heat transfer capacity and the efficiency of ORC between each working fluid by theoretical formulas.

2.0 MODELING AND EXPERIMENTAL SECTION

2.1 Simulation of ORC Thermodynamic Cycle

To start the simulation of ORC thermodynamic cycle by HYSYS using the initial data shown in Table 1 is necessary. As shown in this table the working fluids should be in the subcooled liquid and normal working condition to start the ORC simulation.

Table 1 Initial data needed to simulate ORC in HYSYS

Initial Parameter	Value
Mass Flow Rate, $\dot{m}_{ORC}$ [Kg/h]	15×10^6-30×10^6
Phase Fraction of Working Fluid (Inlet of Separator, Outlet of Pump, Outlet of Cooler)	0
Phase Fraction of Working Fluid (Outlet of Heat Exchanger, Inlet and Outlet of Fluegas, Outlet of Expander)	1
Initial Mole Fraction of Working Fluid	0.9
Initial Mole Fraction of H_2O	0.1
Mole Fraction of Fluegas (H_2O, CO_2, N_2, O_2)	0.19, 0.09, 0.7, 0.02
Initial Temperature (Inlet of Separator),T_i [^{0}C]	5
Temperature (Inlet of Fluegas), $T_{Fluegas\ in}$ [^{0}C]	200
Temperature (Outlet of Fluegas), $T_{Fluegas\ out}$ [^{0}C]	80
Initial Pressure (Inlet of Separator), P_i [KPa]	101.3
Pressure (Outlet of Pump), $P_{outlet\ of\ pump}$ [KPa]	250
Pressure (Outlet of Heat Exchanger), $P_{outlet\ of\ H.E}$ [KPa]	200
Pressure (Outlet of Expander), $P_{inlet\ of\ Ex}$ [KPa]	180
Pressure (Outlet of Cooler), $P_{outlet\ of\ Cooler}$ [KPa]	101.3

As can be seen from Figure 1, first of all, in the present ORC thermodynamic cycle, which is simulated by HYSYS software, working fluids streams are not completely pure and have small amounts of mole fraction of H_2O (90% working fluid and 10% H_2O). For purification to increase the mole fraction of working fluids, in subcooled liquid, normal, and steady state working condition, in 15×10^6 - 30×10^6 Kg/h as range of mass flow rate at liquid phase (phase fraction = 0), working fluids transfer to a separator (S-100). Then working fluids enter the Heat Stream Pump (P-100) to adjust the fluid flow from laminar flow to turbulent flow and increase the pressure of working fluids to 250KPa. Then, working fluids enter the shell and tube Heat Exchanger (H.E-100), to exchange the phase of these working fluids from liquid to gas, which needs a heat source named Fluegas of Boilers. Fluegas has 160 - 240^{0}C range of temperature but as a control temperature of inlet stream of Fluegas, set to 200^{0}C and as a control temperature of outlet stream of Fluegas, set to 80^{0}C. In the present shell and tube Heat Exchanger the temperature of each working fluid is increased but the pressure of each working fluid is reduced to 200KPa. After the exit of these working fluids from this heat exchanger (H.E-100), working fluids in gas phase enter the Expander (E-100) where they cause the rotation of the seal shaft to produce the Electricity energy. The pressure of working fluids at the Expander decreases to 180KPa. Following the exit of these working fluids from the Expander, and then in order to recover these working fluids, and return them to the present ORC thermodynamic cycle, involves changing the phase of these working fluids from gas to liquid. This is to be used again in the ORC thermodynamic cycle to enter the Cooler (C-100) which is working by refrigerant fluid or cooling water in terms of kinds of working fluid. In this equipment the temperature and pressure of each working fluid revert to the pressure and temperature at the first section of ORC system.

2.2 Advantages of Applying Recycle (RCY-1) to Close Current ORC

The last equipment in the present ORC thermodynamic cycle is Recycle (RCY-1). This exclusive equipment is applied for a number of important reasons, such as closing the ORC thermodynamic cycle without any error in each equipment and with the present ORC becoming reversible for recycling the working fluids. It also involves setting the initial temperature of each working fluid stream at the first section of ORC at the inlet of the separator to near their boiling point temperature to increase the efficiency of the ORC, and enhance the performance of shell and tube Heat Exchanger (H.E-100), and to decrease the period of standing of each working fluid at H.E-100 to prevent deposition and pressure drop at H.E-100. Another reason to use this RCY-1 is the function of the Separator, in dewatering from working fluid stream at the first section of ORC system that is increasing the mole fraction of each working fluid from 0.9 to 0.9998 and decreasing the mole fraction of water of each working fluid from 0.1 to 0.0002.

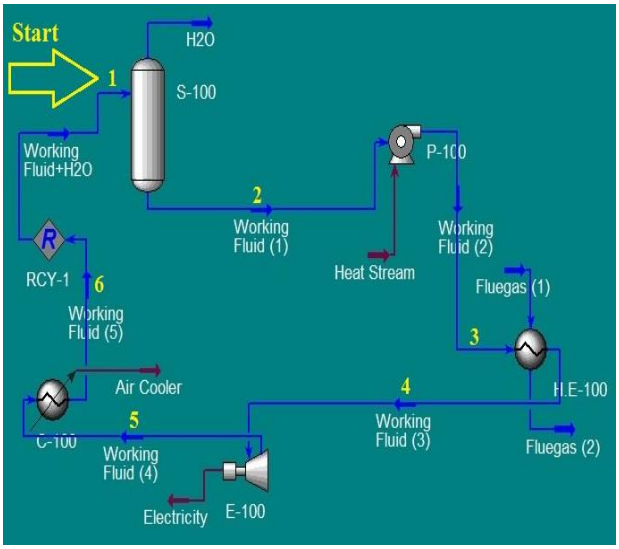

Figure 1 Schematic of ORC Process Driven By R245fa, NOVEC7000 and R141b as Working Fluids

2.3 T-S Diagram of ORC

Figures 2, 3, and 4 illustrate the effects of differences of temperature on Entropy at each component of the present ORC system for R245fa, NOVEC7000, and R141b as working fluids, respectively. According to the slope of the saturation vapor curve on the T-S diagram (dT/dS), the working fluids can be classed as wet, isentropic or dry fluids. For wet fluids, the vapor saturation curve has a negative slope, resulting in a two-phase mixture upon isentropic expansion. Dry fluids have a positive slope, while saturated vapor curve of an isentropic fluid is a nearly vertical line (Expander line). Also, after defining ε= dS/dT, the types of working fluids can be predicted. That is, ε < 0: a wet fluid, ε ~ 0: an isentropic fluid, and ε > 0: a dry fluid. ε can be calculated by using the Eq. (1) presented in [14].

$$\varepsilon = \frac{C_{p_{inlet\ of\ H.E}}}{T_{outlet\ of\ H.E}} - \frac{(n.T_{r_H})/(1-T_{r_H})+1}{T^2{}_{outlet\ of\ H.E}}\Delta H_{H.E} \qquad (1)$$

where ε is the inverse of the slope of the saturated vapor curve on the T-S diagram, $T_{rH}(=\frac{T_{outlet\ of\ H.E}}{T_{outlet\ of\ Cooler}})$ denotes the reduced Heat Exchanger temperature, $\Delta H_{H.E}$ represents the enthalpy of vaporization, and n is suggested to be 0.375 or 0.38 [15]. Equation ε and slope of saturation line can be classified as R245fa, NOVEC7000, and R141b as working fluids of current ORC as mentioned in Table 2.

Table 2 Classification of R245fa, NOVEC7000, and R141b as working fluids in terms of equation

Working Fluids	$T_{outlet\ of\ H.E}$ (°C)	$T_{outlet\ of\ cooler}$ (°C)	T_{rH} (°C)	$C_{p\ inlet\ of\ H.E}$	$\Delta H_{H.E}$ (Kj/Kg)	ε	Type
R245fa	33.40	14.69	2.274	0.696	200	0.586	Isentropic
NOVEC7000	54.40	33.67	1.616	0.6244	139	-0.0636	Isentropic
R141b	53.03	31.62	1.677	0.8288	231	-0.146	Isentropic

Figure 2 shows R245fa as working fluid, process 1-2 is the isothermal and isobaric dewatering process in the Separator. Following that, Process 2-3 is the compression process that is near to isentropic at Pump, but the state point 2' shows the isentropic process of the working fluid at Pump.

However, Figures 3 and 4 reveal the T-S diagrams for the current ORC, which is driven by NOVEC7000 and R141b as working fluids. Process 1-2 is the isothermal, isobaric, and isentropic dewatering process in the Separator. After that Process 2-3 is the isentropic compression process at Pump. Then, in terms of Figures 2, 3 and 4, process 3-4 is the working fluids stream at shell and tube Heat Exchanger, and process 4-5 illustrates the working fluid stream at Expander, and the stream of each working fluid at this instrument is the same as the pump which is near to Isentropic.

However, the state point 5' shows the isentropic process of the working fluid at the Expander. And the state point 5 shows the superheated vapor condition of the working fluid. Also, the state point 6 is located at the saturated vapor line. Process 5-1 indicates the working fluid at Cooler and Recycle. These state points are calculated by HYSYS simulation software.

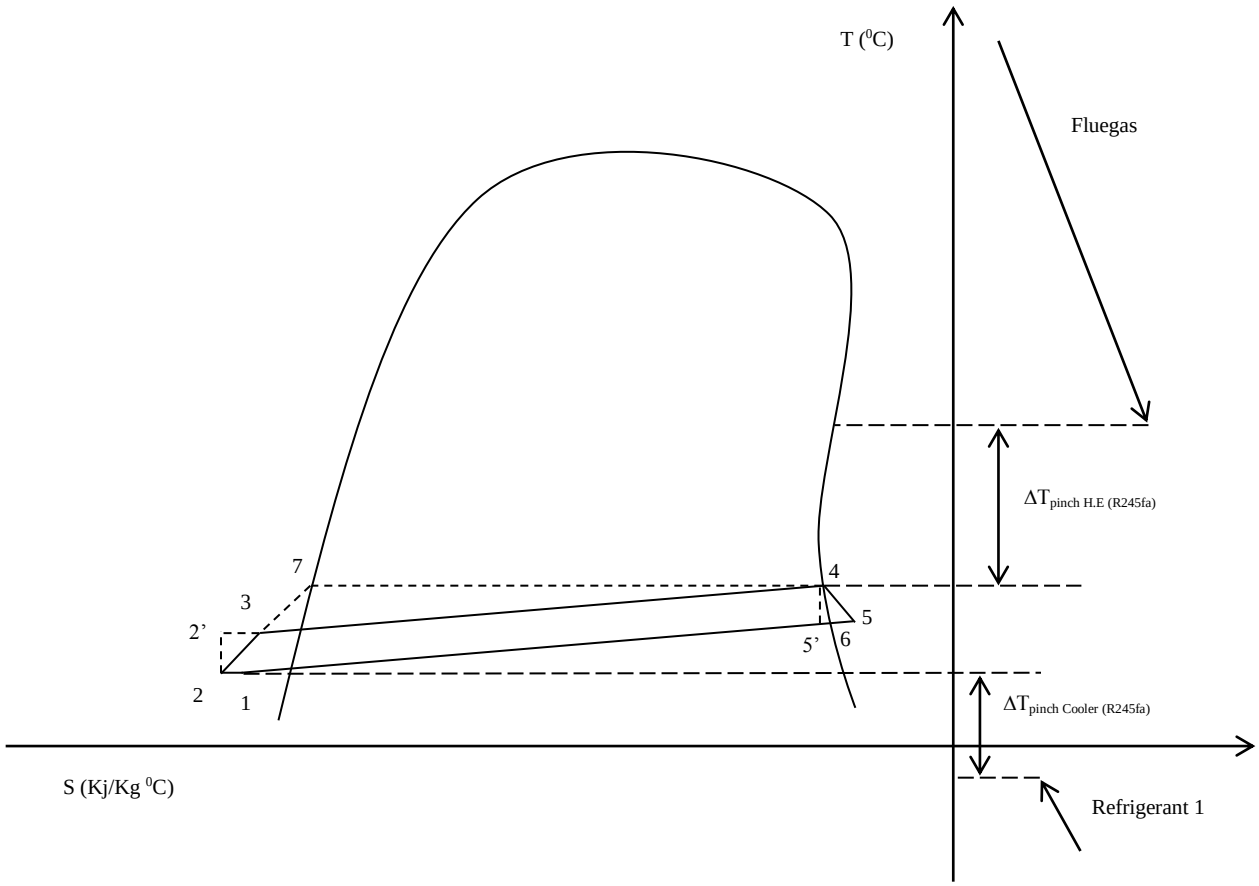

Figure 2 T-S Diagram of ORC for R245fa

The following pinch temperature differences are from these T-S diagrams:

$\Delta T_{pinch\ H.E\ (R245fa)} = 46.62^0C$

$\Delta T_{pinch\ Cooler\ (R245fa)} = 38.69^0C$

$\Delta T_{pinch\ H.E\ (NOVEC7000)} = 25.6^0C$

$\Delta T_{pinch\ Cooler\ (NOVEC7000)} = 8.67^0C$

$\Delta T_{pinch\ H.E\ (R141b)} = 26.97^0C$

$\Delta T_{pinch\ Cooler\ (R141b)} = 6.62^0C$

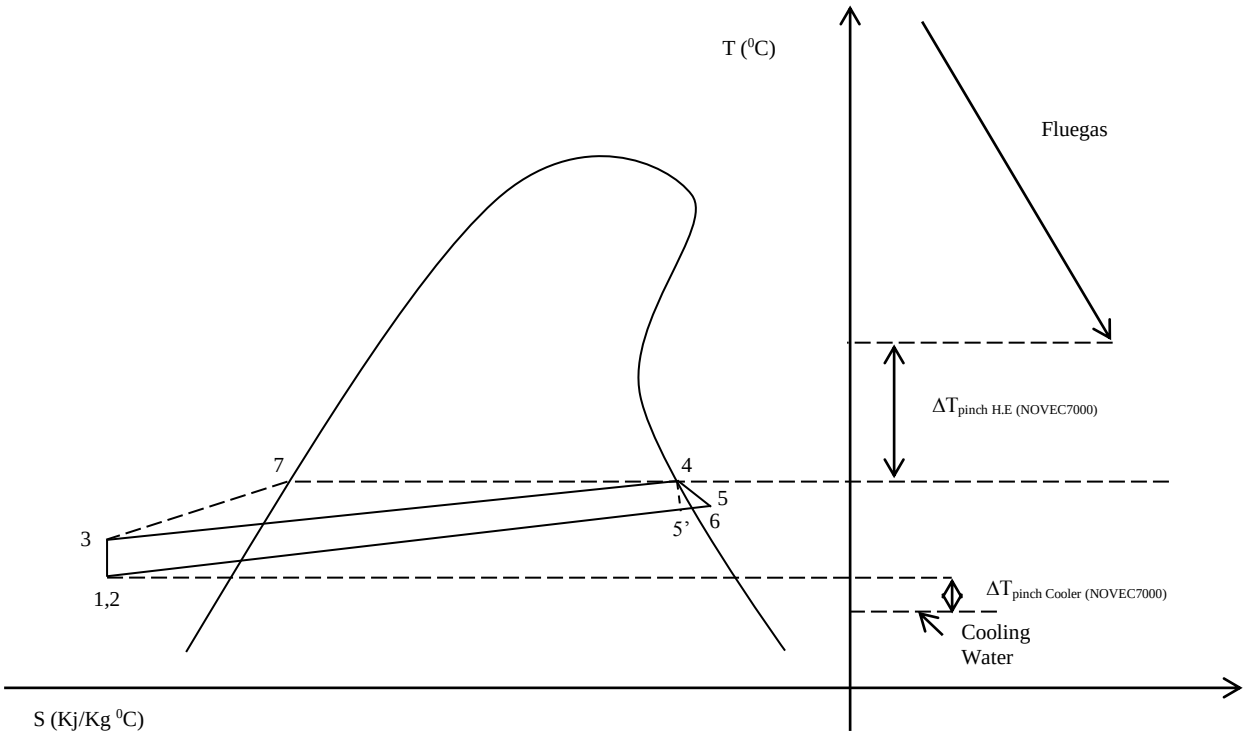

Figure 3 T-S Diagram of ORC for NOVEC7000

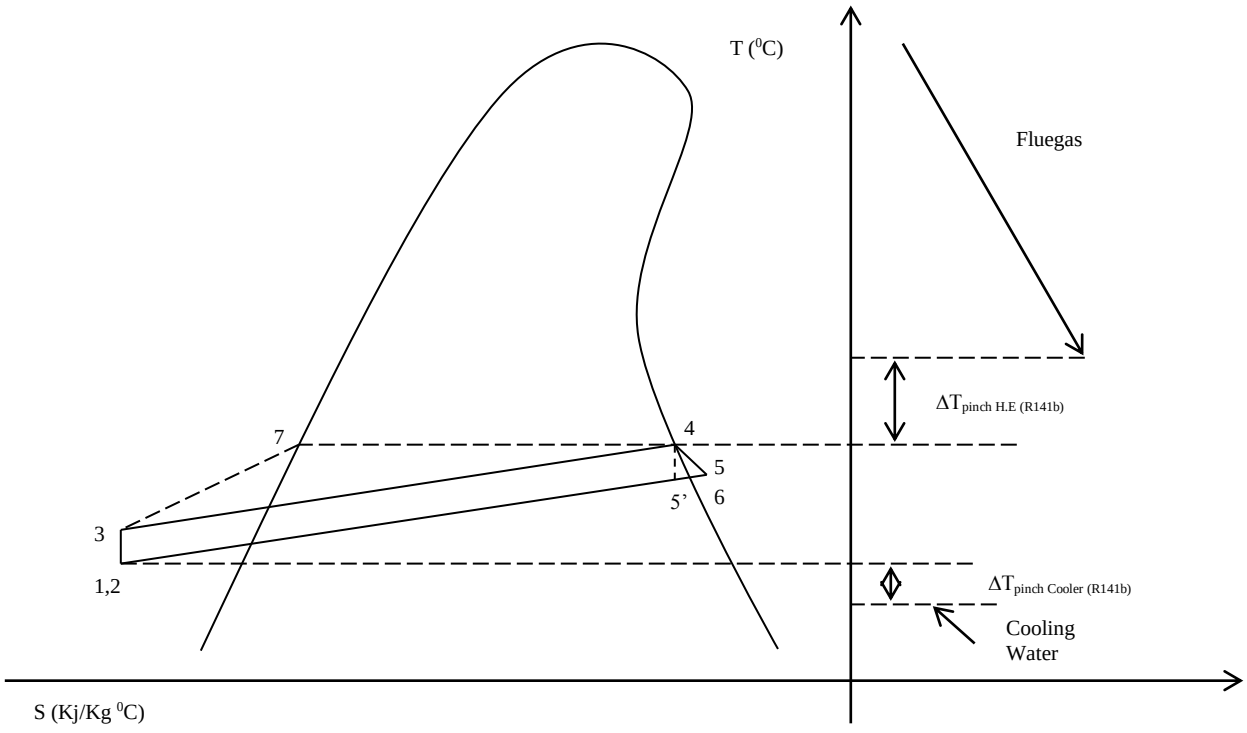

Figure 4 T-S Diagram of ORC for R141b

3.0 THE THEORETICAL FORMULAS OF ORC

3.1 Total Heat Transfer Capacity $(UA)_{total}$

The total heat transfer capacity $(UA)_{total}$, which has been used to evaluate the cost of heat exchangers, can approximately reflect the total heat transfer area of heat exchangers in the ORC system [16,17]. The $(UA)_{total}$ could be evaluated by the following equations:

$$(UA)_{total} = \frac{\dot{Q}_{H.E}}{\Delta T_{H.E}} + \frac{\dot{Q}_{cooler}}{\Delta T_{cooler}} \quad (2)$$

$$\dot{Q}_{H.E} = \frac{dh_{H.E}}{dt} = \dot{m_{W.F}}(h_{outlet} - h_{inlet}) \quad (3)$$

$$\dot{Q}_{cooler} = \frac{dh_{Cooler}}{dt} = \dot{m_{W.F}}(h_{inlet} - h_{outlet}) \quad (4)$$

$$\Delta T_{H.E} = T_{outlet} - T_{inlet} \quad (5)$$

$$\Delta T_{cooler} = T_{inlet} - T_{outlet} \quad (6)$$

where $(UA)_{total}$ is the total heat transfer capacity, $\dot{Q}_{H.E}$ and $\dot{Q}_{cooler}$ are the heat rates injected and rejected, respectively, $\Delta T_{H.E}$ and ΔT_{cooler} are the maximal and minimal temperature differences at the heat exchanger and cooler, respectively.

3.2 Total Efficiency of ORC (η_{ORC})

The second law of thermodynamics limits the maximum efficiency that can be achieved with low temperature of waste heat streams (Fluegas). When heat is added at a constant temperature, e.g. when a latent heat source is available, the total maximum efficiency of ORC, is determined by the Carnot cycle efficiency:

$$\eta_{ORC} = \frac{T_{outlet\ of\ H.E} - T_{outlet\ of\ Cooler}}{T_{outlet\ of\ H.E}} = 1 - \frac{T_{outlet\ of\ Cooler}}{T_{outlet\ of\ H.E}} \quad (7)$$

where η_{ORC} is the total maximum efficiency of ORC. $T_{outlet\ of\ H.E}$ is the absolute temperature at which heat is absorbed (it means at the outlet of Heat Exchanger), and $T_{outlet\ of\ Cooler}$ is the absolute temperature at which heat is rejected (it means at the outlet of Cooler). Lars and William [18] also used this equation.

4.0 RESULT AND DISCUSSION

The net power output of the Expander is different for each working fluid, which drives ORC at the same condition and same thermodynamic characteristics as shown in Figure 5 for R245fa, NOVEC7000, and R141b as working fluids of ORC. These working fluids are dry and contain 0.9 mole fraction pure working fluids and 0.1 mole fraction water at section 1; it means at the inlet of the separator. The highest range of net power output of the Expander is about 6766KW to 13530KW when R141b is adopted. The middle net power output of the Expander is about 4409KW to 8817KW corresponding to NOVEC7000, and the lowest net power output, which belongs to R245fa, has a range between 3204KW and 6408KW. One of the foremost reasons for explaining different net power outputs of the Expander at different specific mass flow rates of different working fluids is that it can be deduced that the larger net power output will be produced when the critical temperature of the working fluid approaches the temperature of the waste heat source. For adopting this reason with current results which are shown in Figure 5, reference should be made to the critical temperature of R141b, NOVEC7000, and R245fa which are assigned at 204.1°C, 165°C, and 154°C, respectively. Furthermore, the temperature of Fluegas at inlet of Heat Exchanger is 200°C, and it means the highest, middle, and lowest amounts of net power output of the Expander should belong to R141b, NOVEC7000, and R245fa. These results, in terms of the above reason are in agreement with the results of Hysys simulation of the present ORC, as shown in Figure 5. Another but less important reason is the Polytropic efficiency of the Expander.

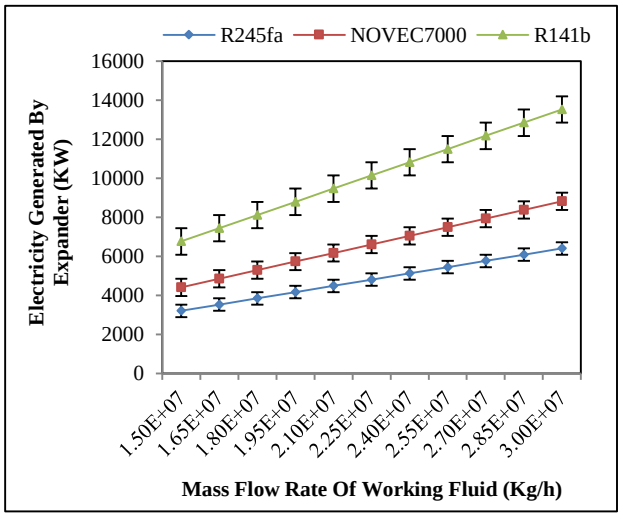

Figure 5 The net power output of Expander of ORC thermodynamic cycle at different specific mass flow rates of different working fluids. Error bars represent standard errors of the mean

This thermodynamic parameter has a linear relationship with the net power output of the Expander of the ORC thermodynamic cycle at different specific mass flow rates of different working fluids. In terms of investigating the Polytropic efficiency of working fluids at the Expander, R245fa has the lowest Polytropic efficiency at the Expander, and has the lowest amount of power generated at the Expander. All in all, in the present study, the best

choice of working fluids in terms of net power generated by the Expander is R141b. This result is similar to Chao *et al.* [19].

Figure 6 compares the optimum pressure of working fluids at the inlet of the Expander and the temperature of the working fluids at the inlet of the Expander; whereas, the optimum pressure of working fluids at the inlet of the Expander has a linear relationship with the temperature of the working fluids at the inlet of the Expander. As shown in Figure 7, the optimum pressure of working fluids at the inlet of the Expander has a positive strong correlation on the amount of electricity generated by the Expander and also the power generated by the cooler and as a result the net power output of the ORC. As shown in Figure 6 the highest, middle, and lowest temperatures of working fluids at the inlet of Expander are NOVEC7000, R141b, and R245fa, respectively. And also for Electricity generated by the Expander, the highest, middle, and lowest are R141b, NOVEC7000, and R245fa, respectively.

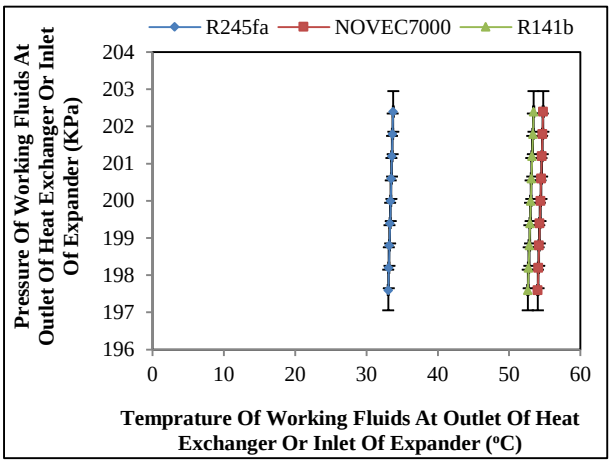

Figure 6 The impact of optimum pressure of working fluids at inlet of Expander with temperature of working fluids at inlet of Expander. Error bars represent standard errors of the mean

Due to the fact that in the present ORC thermodynamic cycle, after closing the cycle with the Recycle instrument, the temperature of each working fluid is set to near the boiling point of each working fluid to increase the efficiency and economy of the heat exchanger and also the present ORC thermodynamic cycle; hence ,sometimes for a number of refrigerant working fluids which have greater differences of thermal energy among each other, the thermal energy converts to electrical energy in the Expander and this is one of the important reasons for the different levels of electricity generated in the Expander by R245fa, NOVEC7000, and R141b as working fluids. To sum up, the suitable choices and selection of working fluids are R141b and NOVEC7000. These results are similar to reported results by [11] who worked on Trans-critical Rankine Cycle (TRC systems) driven by some zeotropic mixture of working fluids.

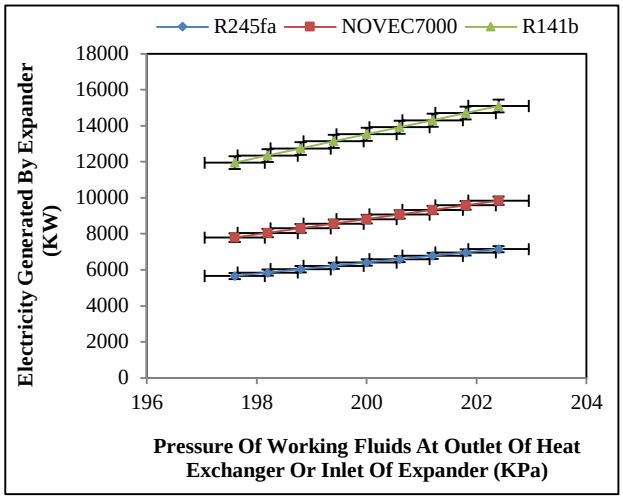

Figure 7 The impact of optimum pressure of working fluids at inlet of Expander with electricity generated by Expander. Error bars represent standard errors of the mean

Figure 8 illustrates the total heat transfer capacity $(UA)_{total}$ for R245fa, NOVEC7000, and R141b as working fluids at minimum mass flow rates and maximum mass flow rates of working fluids, respectively. Usually, the higher total heat transfer capacity $(UA)_{total}$ means a higher cost of the heat exchanger. As shown in Figure 8 the total heat transfer capacities for R245fa, NOVEC7000, and R141b are 9.78×10^4 KW/^{0}C, 6.15×10^4 KW/^{0}C, and 9.86×10^4 KW/^{0}C, respectively, at minimum mass flow rates of working fluids and 1.96×10^5 KW/^{0}C, 1.23×10^5 KW/^{0}C, and 1.97×10^5 KW/^{0}C, respectively, at maximum mass flow rates of working fluids. Current results indicate that R141b is highest and NOVEC7000 is the lowest, but in terms of these results the total heat transfer capacity for R245fa is middle and near to R141b. The first and foremost reason for the increase and decrease of the total heat transfer capacity $(UA)_{total}$ ot these different working fluids is the temperature differences of the heat exchanger and cooler ($\Delta T_{H.E}$ and ΔT_{cooler}). Because this thermodynamic parameter has an inverse correlation with temperature differences of the heat exchanger and cooler; in the present ORC thermodynamic cycle, after closing the cycle by Recycle instrument, the temperature of each working fluid is set to near the boiling point of each working fluid. This is to increase the efficiency and economy of the heat exchanger and also present the ORC thermodynamic cycle. The second important reason is that it can be more influential in changing the $(UA)_{total}$ for R245fa, NOVEC7000, and R141b as working fluids in mass enthalpy of working fluids at heat exchanger and cooler ($\Delta h_{H.E}$ and Δh_{cooler}) with linear relationship. The last effective reason for going up and going down of each column of Figure 8 is the mass flow rate of working fluids before the heat

exchangers. Because the mass flow rate of working fluids ($\dot{m}_{W.F}$) has a linear correlation with total heat transfer capacity $(UA)_{total}$, it means with increase in the ($\dot{m}_{W.F}$) , $(UA)_{total}$ also increases. All in all, the best choice and selection for the present ORC thermodynamic cycle in terms of economic considerations and cost of heat exchangers, is NOVEC7000. However, the net power output of ORC and total efficiency of ORC are not ideal for this working fluid. Similar responses have been reported in another ORC system which was simulated and analyzed with EES (Engineering Equation Solver) by Chao *et al.* [19].

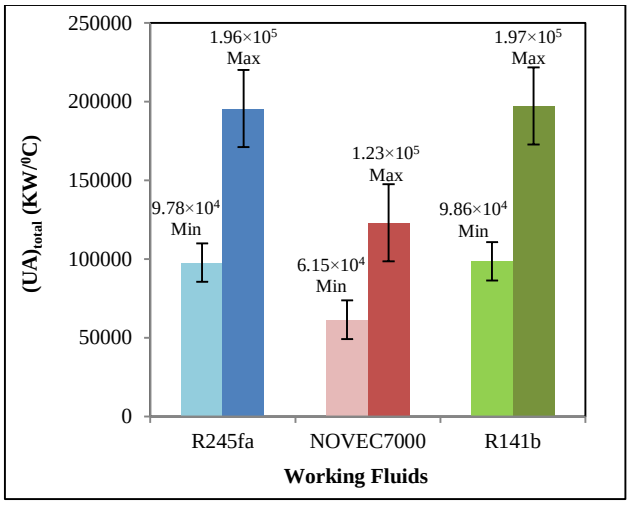

Figure 8 The total heat transfer capacity $(UA)_{total}$ of the ORC with different working fluids at minimum and maximum mass flow rates of working fluids.. Error bars represent standard errors of the mean

The total efficiency of ORC for R245fa, NOVEC7000, and R141b at different specific inlet pressures of Expander (E-100) can be found in Figure 9, where the results indicate that the highest, middle, and lowest efficiencies of ORC belong to R245fa, R141b, and NOVEC7000, with mean value of 56.01%, 40.37%, and 38.10%, respectively. According to Figure 9, by increasing the inlet pressure of Expander (E-100) from 197.6KPa, to 202.4KPa, the inlet temperature of Expander (E-100) is increased dramatically. Hence, increasing the inlet pressure of Expander leads to increase of the inlet temperature of Expander and as a result can increase the total efficiency of ORC for R245fa, NOVEC7000, and R141b as working fluids. The total efficiency of ORC is based on two thermal parameters, the outlet temperature of Cooler (C-100) and outlet temperature of shell and tube Heat Exchanger (H.E-100). Furthermore, the most important parameter that plays a pivotal role in the differences among working fluids is bubble point temperature of each working fluid. This thermal parameter (bubble point temperature of each working fluid) has an inverse linear relation with the efficiency of ORC. Therefore, the results suggest that, the best and more suitable choice of working fluids in terms of ORC efficiency is R245fa. These results concur with Naijun *et al.* [20] who worked on the experimental system for heat recovery from low-temperature Fluegas based on the constructed Organic Rankine Cycle (ORC). In the system, R123 was selected as the working fluid, and a scroll expander was used to produce work, and fine tubes heat exchanger was designed as the evaporator. Low-temperature Fluegas produced by a liquefied petroleum gas (LPG) stove was used as the heat source to simulate industrial Fluegas, and its temperature can be controlled within the range of 90^0C - 220^0C. Also, this result is in agreement with that of another result by Seok *et al.* [21] who used the ORC system with a radial turbine that was directly connected to a high-speed synchronous generator.

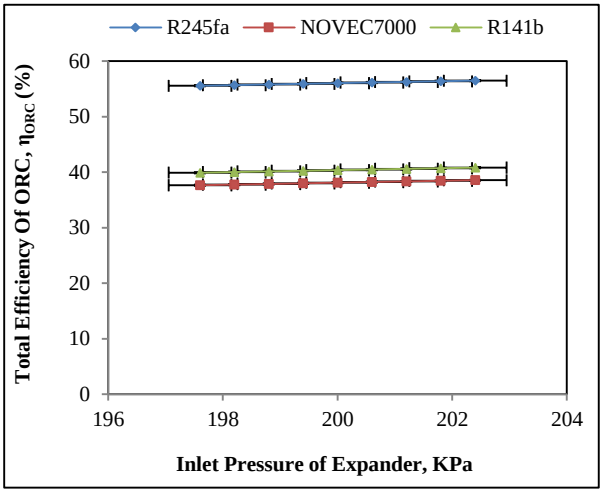

Figure 9 The influence of different specific inlet pressures of Expander (E-100) on the total efficiency of ORC driven by R245fa, NOVEC7000, and R141b, respectively. Error bars represent standard errors of the mean

5.0 CONCLUSION

The present study was carried out to investigate and simulate the ORC thermodynamic cycle by using R245fa, NOVEC7000, and R141b as refrigerant working fluids and driven by Fluegas by using HYSYS to generate large scale electricity. In this study, inlet pressure of Expander (197.6KPa - 202.4Kpa) and mass flow rates of working fluids before Separator (15×10^6 - 30×10^6 Kg/h) play pivotal roles in generating large scale Electricity at Expander. On the other hand, the maximum net electricity power output from Expander was generated when critical temperature of each working fluid approach to the inlet Fluegas temperature; therefore, the highest range of net power output of the Expander is about 6766KW to 13530KW when R141b is adopted. The middle net power output of the Expander is about 4409KW to 8817KW corresponding to NOVEC7000, and the lowest net power output which belongs to R245fa, has a range between 3204KW and 6408KW.

Furthermore, the total heat transfer capacity $(UA)_{total}$, affected by different mass flow rates of working fluids, and in terms of economic consideration and cost of heat exchangers, NOVEC7000 was the optimum selection in current research. But in terms of total efficiency of ORC, NOVEC7000 was not an ideal choice because of lowest efficiency (38.10%) compared with other working fluids. Therefore, R245fa with 56.01% total efficiency, is the best and more suitable choice of working fluids for the present ORC in the current study.

References

[1] Qiu, G. 2012. Selection of working fluids for micro-CHP systems with ORC. *Renew- able Energy*. 48: 565–570.

[2] Wei, D., Lu, X., Lu, Z. and Gu, J. 2007. Performance analysis and optimization of organic Rankine cycle (ORC) for waste heat recovery. *Energy Conversion and Management*. 48: 1113-1119.

[3] Quoilin, S., Lemort, V. and Lebrun, J. 2010. Experimental study and modeling of an Organic Rankine Cycle using scroll expander. *Applied Energy*. 87: 1260-1268.

[4] DiPippo, R. 2004. Second law assessment of binary plants generating power from low-temperature geothermal fluids. *Geothermics*. 33: 565–586.

[5] Wang, E. H., Zhang, H. G., Fan, B. Y., Ouyang, M. G., Zhao, Y. and Mu, Q. H. 2011. Study of working fluid selection of organic Rankine cycle (ORC) for engine waste heat recovery. *Energy*. 36: 3406–3418.

[6] Yamamoto, T., Furuhata, T., Arai, N. and Mori, K. 2001. Design and testing of the Organic Rankine Cycle. *Energy*. 26: 239-251.

[7] Kang, H. 2009. Organic Rankine cycle technology. *Journal of the KSME*. 49: 47-52.

[8] Dai, Y. P., Wang, J. F. and Lin, G. 2009. Parametric optimization and comparative study of organic Rankine cycle (ORC) for low grade waste heat recovery. *Energy Conversion and Management*. 50: 576-582.

[9] Pei, G., Li, J., Li, Y., Wang, D. and Ji, J. 2011. Construction and dynamic test of a small-scale organic Rankine cycle. *Energy*. 36: 3215-3223.

[10] Hun, K. 2012. Design and experimental study of ORC (Organic Rankine Cycle) and radial turbine using R245fa working fluid. *Energy*. 41: 514–524.

[11] Baomin, D., Minxia, L. and Yitai, M. 2014. Thermodynamic analysis of carbon dioxide blends with low GWP (global warming potential) working fluids-based transcritical Rankine cycles for low-grade heat energy recovery. *Energy*. 64: 942–952.

[12] Karellas, S., Schuster, A. and Leontaritis, A. 2012. Influence of supercritical ORC parameters on plate heat exchanger design. *Applied Thermal Engineering*. 33–34: 70–76.

[13] Sebastian, D., Sylvain, Q. and Vincent, L. 2010. Design and experimental Investigation of a small scale Organic Rankine Cycle using a Scroll Expander. *Refrigeration and Air conditioning Int. Conference*. Purdue University.

[14] Liu, B. T., Chien, K. H. and Wang, C. C. 2004. Effect of working fluids on organic Rankine cycle for waste heat recovery. *Energy*. 29: 1207-1217.

[15] Bruce E. Poling, Prausnitz M. Prausnitz and John P. O'Connell. 2000. The properties of gases and liquids, fifth ed., New York: McGraw- Hill Professional.

[16] Guo, T., Wang, H. X. and Zhang, S. J. 2011. Comparative analysis of natural and conventional working fluids for use in transcritical Rankine cycle using low-temperature geothermal source. *International Journal of Energy Resource*. 35: 530-544.

[17] Schuster, A., Karellas, S. and Aumann, R. 2010. Efficiency optimization potential in supercritical Organic Rankine Cycles. *Energy*. 35: 1033-1039.

[18] Lars, J. B. and William, M. B. 2004. Ranking of Working Fluids for Organic Rankine Cycle Applications. *International Refrigeration and Air Conditioning Conference, School of Mechanical Engineering.* Purdue University Purdue e-Pubs.

[19] Chao, H. C., Liu, C., Gao, H., Xie, H., Li, Y., Wu, S. and Xu, J. 2012. The optimal evaporation temperature and working fluids for subcritical organic Rankine cycle. *Energy*. 38: 136–143.

[20] Naijun, Z., Xiaoyuan, W., Zhuo, C. and Zhiqi, W. 2013. Experimental study on Organic Rankine Cycle for waste heat recovery from low-temperature flue gas. *Energy*. 55: 216–225.

[21] Seok, H. K. 2012. Design and experimental study of ORC (Organic Rankine Cycle) and radial turbine using R245fa working fluid. *Energy*. 41: 514–524.

Nomenclature

Symbols		T_{inlet}	Inlet temperature (^{0}C)
ORC	Organic Rankine Cycle	T_{outlet}	Outlet temperature (^{0}C)
Δh_{vap}	Heat of vaporization (Kj/Kg)	$T_{outlet\ of\ H.E}$	Absolute temperature at which heat is absorbed (it means at the outlet of Heat Exchanger) (^{0}C)
ρ_{vap}	Density in vapor state (Kg/m^3)	$T_{outlet\ of\ Cooler}$	Absolute temperature at which heat is rejected (it means at the outlet of Cooler) (^{0}C)
P_c	Critical pressure (KPa)	**Greek Symbol**	
V_c	Critical volume (m^3)	η_{ORC}	Total maximum efficiency of ORC
$\Delta T_{pinch\ H.E\ (R245fa)}$	The pinch temperature difference in Shell and Tube Heat Exchanger for R245fa (^{0}C)	**Subscript**	
$\Delta T_{pinch\ Cooler\ (R245fa)}$	The pinch temperature difference in Cooler for R245fa (^{0}C)	*H.E*	Shell and tube Heat Exchanger
$\Delta T_{pinch\ H.E\ (NOVEC7000)}$	The pinch temperature difference in Shell and Tube Heat Exchanger for NOVEC7000 (^{0}C)	*Ex*	Expander
$\Delta T_{pinch\ Cooler\ (NOVEC7000)}$	The pinch temperature difference in Cooler for NOVEC7000 (^{0}C)	*Net*	Net
$\Delta T_{pinch\ H.E\ (R141b)}$	The pinch temperature difference in Shell and Tube Heat Exchanger for R141b (^{0}C)	*W.F*	Working Fluid
$(UA)_{total}$	Total heat transfer capacity (KW/^{0}C)	*vap*	Vaporization
$\dot{Q_{H.E}}$	heat rate injected (Kj/h)	*b.p*	Boiling Point temperature
$\dot{Q_{cooler}}$	heat rate rejected (Kj/h)	*M.W*	Molecular Weight
$\dot{m_{W.F}}$	Mass flow rate of working fluids (Kg/h)		
h_{outlet}	Outlet Enthalpy (Kj/Kg)		
h_{inlet}	Inlet Enthalpy (Kj/Kg)		